

# Identifying detector crosstalk events in the dark matter signal region of the Super Cryogenic Dark Matter Search

R. S. Fitzpatrick

*Department of Physics, Princeton University, Princeton, NJ 08544*

*Science Undergraduate Laboratory Internship*

*Particle Physics Division, Fermilab, Batavia, IL 60510*

(Dated: 8 August 2014)

Despite the ample evidence that dark matter makes up approximately 85% of the matter in the universe, it has never been detected directly. The Super Cryogenic Dark Matter Search (SuperCDMS) is looking for weakly interacting massive particles (WIMPs) that may interact with germanium nuclei. Capacitance between detectors in SuperCDMS can cause a large charge signal on one detector to generate a smaller, negative pulse on an adjacent detector. If the crosstalk from a neighboring detector reduces the charge signal by enough to reduce the ionization yield significantly, it can look like a nuclear recoil and impede the definition of a WIMP search region. We show that charge crosstalk occurs on the order of 0.5% of the primary signal, then develop a method to identify events being affected by crosstalk and assess its efficiency for identifying crosstalk events in barium calibration data. By requiring that 10% of the actual charge amplitude exceed the crosstalk amplitude we define a robust selection criteria for selecting events. With the removal of these events, the true barium multiples can be used to study the behavior of  $\gamma$ -interactions and define a search region for low-background data.

## CONTENTS

<b>I. Introduction</b>	3
A. Direct detection in SuperCDMS	5
<b>II. Detector-detector crosstalk</b>	7
A. Charge crosstalk	7
1. Crosstalk events	9
2. Noise-like events	10
B. Phonon crosstalk	11
<b>III. A cut to identify crosstalk</b>	11
A. Cut definition	12
B. Performance	14
<b>IV. Conclusions</b>	16
<b>Acknowledgments</b>	17
<b>References</b>	18

## I. INTRODUCTION

Current estimates predict that non-baryonic dark matter makes up approximately 85% of all matter in the universe.<sup>1</sup> There are strong indications of dark matter in the present universe—superstructure of galactic clusters, galaxy dynamics, gravitational lensing—and in features of the primitive universe such as the cosmic microwave background and big bang nucleosynthesis.<sup>2,3</sup> Beyond indicating the existence of dark matter, observations have been used to determine criteria that dark matter candidates must satisfy. It must be non-baryonic; the baryonic matter in the Milky Way has been well documented, and it does not satisfy the conditions for the rotation curve of the galaxy, nor is it plentiful enough to be responsible for the superstructure of the universe.<sup>2</sup> It only interacts with itself and other matter gravitationally as illustrated by the behavior of the Bullet Cluster.<sup>4</sup> It must also be stable; it will not have decayed into new particles since the birth of the universe. Finally, dark matter must be cold. To be consistent with large-scale structure of the universe it has to be moving at non-relativistic velocities.

The Standard Model of particle physics has become one of the most accurate and well-tested models in modern science. It describes the behavior of the baryonic matter and forces in the universe. However, it provides no unique description of the behavior and particle nature of the dark matter in the universe, nor does it require that dark matter be comprised of a single type of particle.<sup>2</sup> Dark matter candidates that have been proposed include, but are not limited to, Standard Model neutrinos, sterile neutrinos, axions, supersymmetric particles, WIMPs, and Kaluza-Klein states.<sup>1,2,5</sup>

The particle nature of dark matter could be identified in three broad categories of experiment. Indirect detection experiments, such as the Fermi Gamma-ray Space Telescope mission<sup>6</sup>, search for annihilation products of dark matter in regions where it is known to exist. There is also the possibility that dark matter particles could be created and detected in accelerators like the LHC. Finally, there are numerous experiments, like SuperCDMS for detecting dark matter particles directly by observing a nuclear recoil from the interaction between a dark matter particle and a large target nucleus.

WIMPs, or weakly interacting massive particles, are one of the most promising candidates for dark matter. The most impressive evidence for their existence is that the relic density of WIMPs in the universe calculated from simple dimensional arguments matches the measured

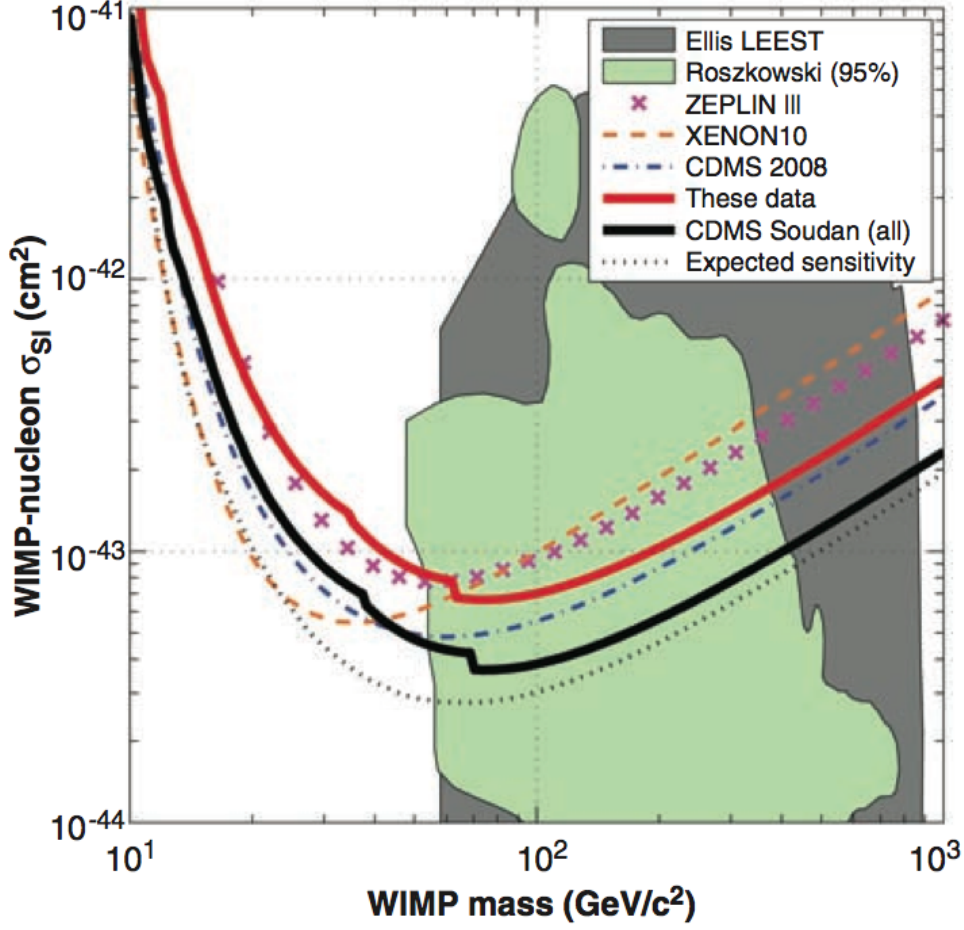


FIG. 1. From Reference 10, 90% confidence upper limit closed contours and exclusion limits defined by many current dark matter experiments including CDMS II, ZEPLIN III, and XENON10. As the curves move toward lower mass and cross-section, the sensitivity of the detectors being created must increase accordingly. SuperCDMS improves upon the methods used in CDMS II to seek definitive evidence for the existence of WIMPs.

amount of dark matter,  $\Omega_{DM} \simeq 0.227$ .<sup>1</sup> This persuading piece of evidence is commonly referred to as the “WIMP Miracle.” The Super Cryogenic Dark Matter Search (SuperCDMS) searches for WIMPs by detecting the nuclear recoil that occurs when a WIMP interacts with baryonic matter. SuperCDMS uses fifteen interleaved Z-sensitive Ionization Phonon (iZIP) detectors, of germanium crystals arranged in five towers, as shown schematically in Figure 2. Despite having not found definitive evidence of WIMPs, the past and current dark matter experiments have restricted the WIMP energy scale. Figure 1 illustrates CDMS II’s results in conjunction with previous results. While CDMS II was able to record three candidate

events, the variation from background noise was not statistically significant, as the estimated background signal was  $0.9 \pm 0.2$  events. SuperCDMS improves upon the methods of CDMS II to increase the sensitivity to WIMP-nucleon interactions.

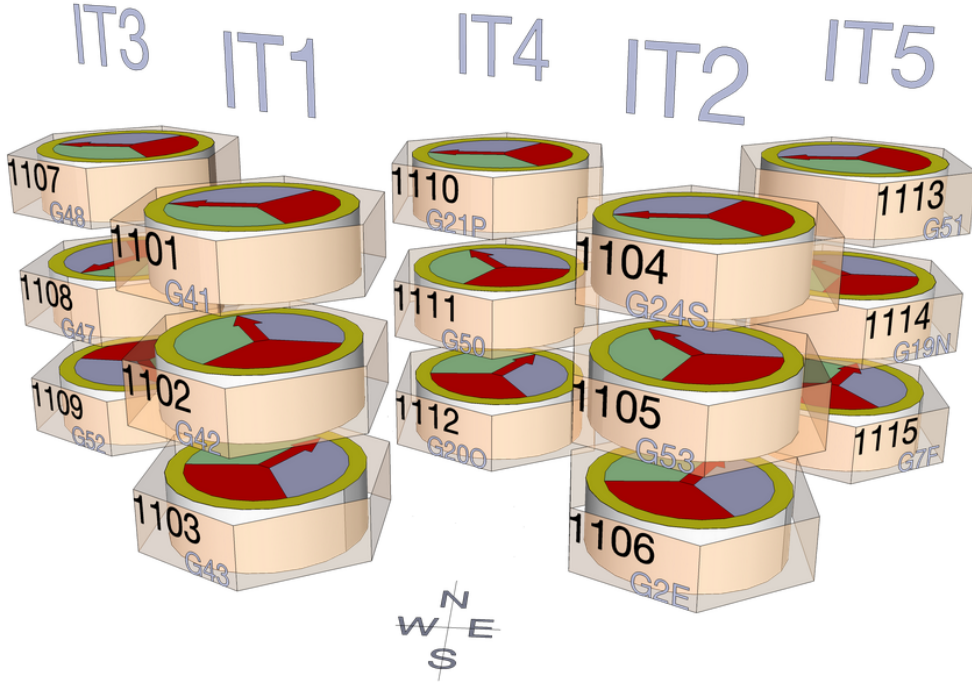


FIG. 2. The layout of the iZIPs in the SuperCDMS detector. The top of each detector is labeled side 1 and the bottom is labeled side 2. Crosstalk measurements are made between side 1 of the lower detector and side 2 of the higher detector. In addition to being labeled 1101, 1102, etc., the detectors can be labeled using the tower (i.e., T1) and the position in the tower – Z1, Z2, Z3 for the top, middle, and bottom detectors. This is the convention that will be used throughout the analysis.

### A. Direct detection in SuperCDMS

SuperCDMS records athermal phonon and ionization information for each event incident on the detectors. Together, the two quantities can be used to distinguish WIMP signatures (nuclear recoil) from electron recoil generated by background events. A nuclear recoil is discriminated from electron recoil signals through ionization yield, the ratio of ionization

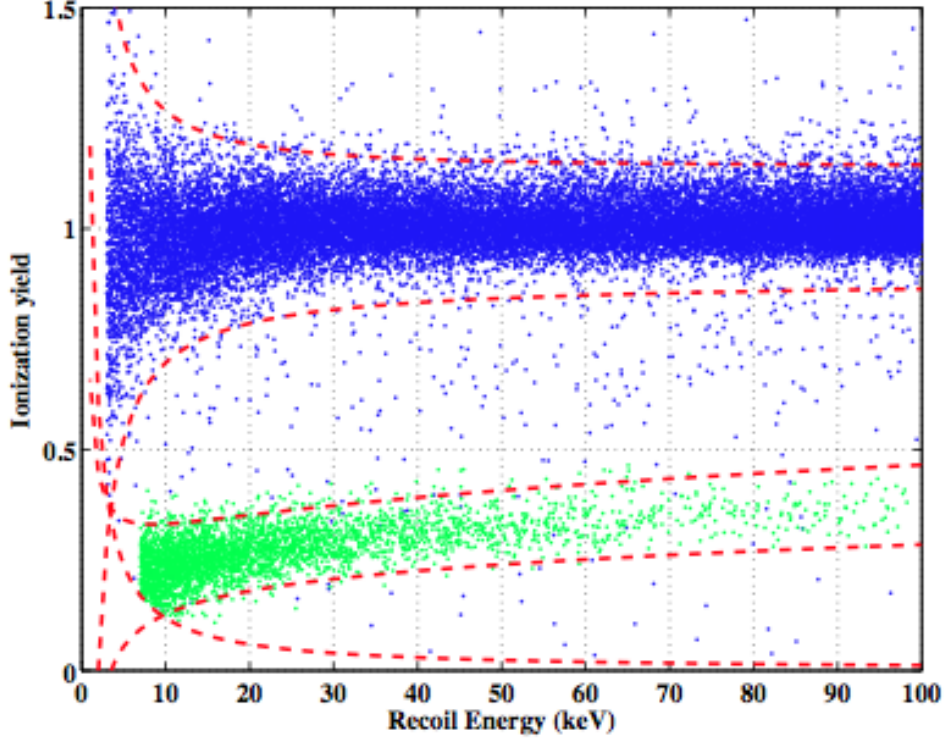


FIG. 3. The  $2\sigma$  nuclear and electron recoil bands generate from  $^{255}\text{Cf}$  and  $^{133}\text{Ba}$  calibration data from Reference 3. The electron recoils are shown in blue, and the nuclear recoils in green. These sources are used to study interactions that may occur in background data.

energy to total recoil energy:

$$y \equiv \frac{E_Q}{E_r} = \frac{E_Q}{E_P - \frac{eV_b}{\epsilon} E_Q} \quad (1)$$

where  $\epsilon$  is the energy that is necessary to generate an electron-hole pair. It is normalized such that  $y = 1$  for electron recoils. Since the ratio of charge amplitude to phonon amplitude is smaller for nuclear recoils, these events fall below the electron recoil band. Figure 3 illustrates the distinct nuclear and electron recoil bands measured using  $^{255}\text{Cf}$  and  $^{133}\text{Ba}$  calibration data, respectively. The calibration datasets are used to study the interactions that may occur in low-background data used to search for WIMP signals. They are used to develop the consistency region for the WIMP search—the area on the yield vs. recoil energy plane where WIMP signals are most likely to fall. Barium events that trigger multiple detectors are used to understand the  $\gamma$ -interactions in low-background data. This requires that we understand all causes of multiple triggers, so they do not bias our understanding of those that resemble  $\gamma$ -interactions, true multiples. When multiples occur on adjacent

detectors, crosstalk between the detectors can alter the signals by enough that an electron recoil could be misinterpreted as a nuclear recoil. This can bias the definition of a WIMP search region, in which the aim is to reduce leakage to less than one event per detector.

## II. DETECTOR-DETECTOR CROSSTALK

Capacitance between the iZIPs can generate negatively charge pulses on detectors adjacent to a triggered detector. In the case of adjacent multiples, if the crosstalk from a second detector reduces the charge signal on the detector being studied by enough to push it into the consistency region, it can be misinterpreted as a true leakage event. This is evident from the form of Equation 2. If  $E_Q$  is reduced by crosstalk, the ionization yield will decrease, pushing the event below the electron recoil band toward the nuclear recoil band. Though multiples are removed from the low-background data when searching for WIMP signatures, they are used to define an accurate consistency region for WIMP search. Crosstalk can affect the behavior of multiples and inhibit the development of an accurate consistency region by artificially reducing ionization yield.

Here we examine the charge crosstalk between all adjacent detectors to design a cut to remove electron recoil events that are being pushed into the nuclear recoil band and test its ability to isolate events affected by crosstalk that fall into the consistency region. The goal is to understand the characteristics of crosstalk and measure the strength of the crosstalk between all pairs of adjacent detectors. In addition, we briefly examine phonon-phonon and charge-phonon crosstalk to check whether the cut should include a test of these parameters.

Throughout the analysis, the term “primary detector” is used to describe the detector whose signal generates a small pulse on an adjacent detector. The “crosstalk detector” is the detector of interest.

### A. Charge crosstalk

It was shown in previous studies that crosstalk is on the order of 0.5% of the primary signal.<sup>7</sup> The data, shown in Figure 4 for T3Z1, confirms the calculation. The charge measured on side 2 of T3Z1 is proportional to the charge on side 1 of T3Z2. A 2 MeV pulse of T3Z2 causes a  $-10$  keV pulse on T3Z1.

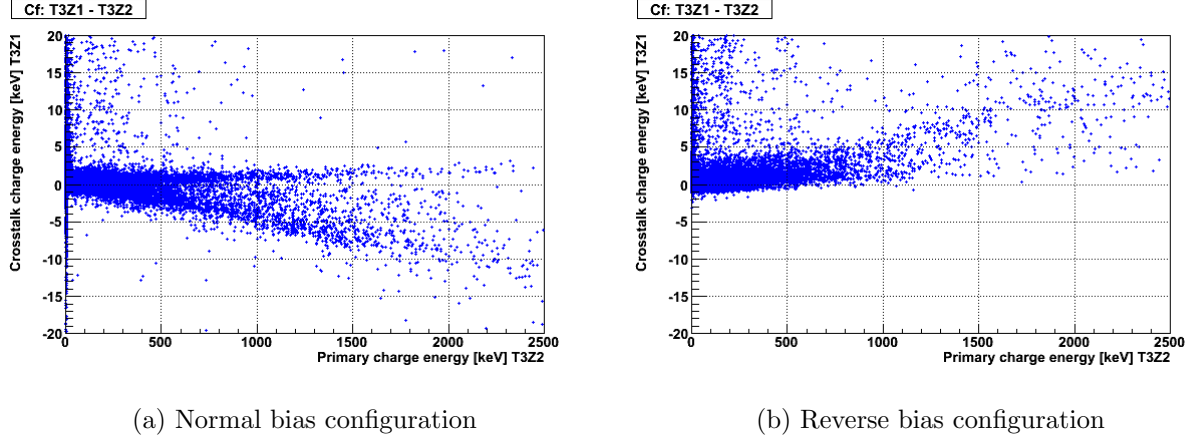


FIG. 4. The crosstalk between two adjacent detectors, where T3Z1 is the crosstalk detector. Rather than having no charge signal for events that trigger the primary detector, the crosstalk detector measures a negative charge signal with strength proportional to the primary signal. There is an additional band of events that remains just above the axis. The cause of these anomalies is illustrated in Figure 6

Crosstalk is most evident between T3Z1 and T3Z2, but most other pairs exhibit the features of crosstalk. Charge crosstalk pulls the band that lies along the primary axis below the axis with a slope of  $< 0.5\%$ . That is, when an event occurs on the primary detector, there should be no charge signal on the adjacent detectors; but charge crosstalk causes a negative pulse proportional to the strength of the primary signal, so the data no longer lies along the axes in the plane relating charge on the two detectors.

In the T3Z1-T3Z2 pair, shown in Figure 4, there is also a band lying above the primary detector axis that mirrors the normal crosstalk band. During R133, the bias on T3Z1 was reversed for certain series for calibration, so that side 1 was  $-2$  V rather than  $+2$  V. The upper band illustrates the data taken during series when the detector was in reverse bias configuration.

To better understand the characteristics of crosstalk, pulses were examined in two regions of Figure 4. First, events in the crosstalk band at very high energies ( $> 5$  MeV) on the primary detector were studied to verify that the original signals match the calibrated quantities illustrated in Figure 4. Second, there are events along the primary detector axis ( $1 - 2$  MeV) with nearly zero energy ( $-2 - 2$  keV) on the crosstalk detector that create a second band distinct from the crosstalk band. It is not clear why these events do not fall



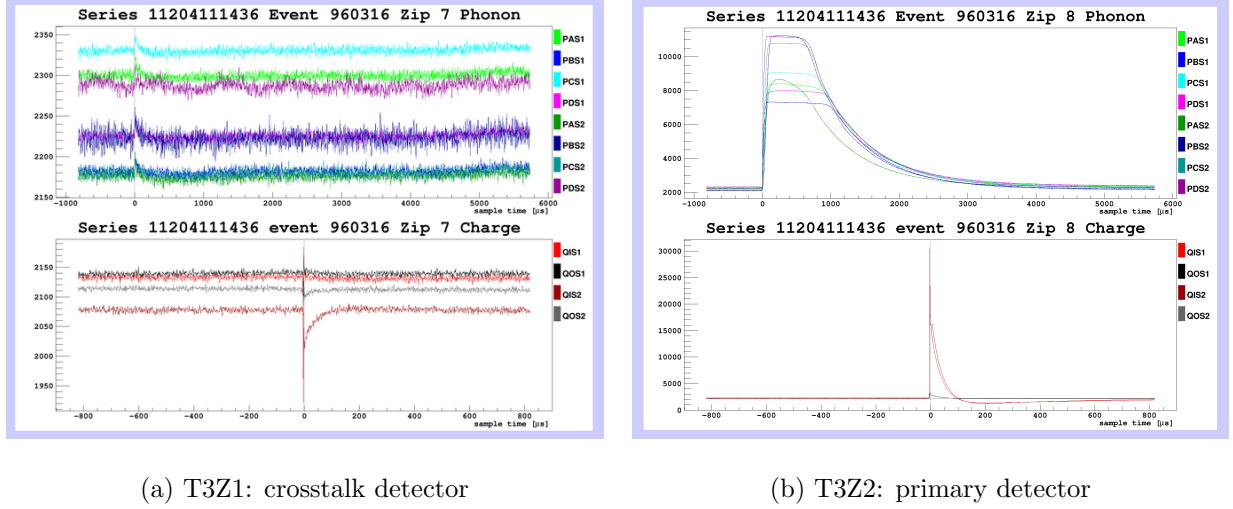


FIG. 5. A crosstalk pulse on T3Z1. The primary pulse on T3Z2 had a charge signal  $> 5$  MeV. The negative charge signal on this detector measured approximately  $-25$  keV. In addition to the charge crosstalk, we also observe a small phonon signal generated by crosstalk between phonon channels or between charge and phonon channels.

within the smear of the crosstalk band, as crosstalk should not distinguish between pulses and affect all signals relatively equally.

### 1. Crosstalk events

A pulse from the crosstalk band is shown in Figure 5, in which characteristic negative charge signal is apparent. If this occurred simultaneously with an event on the crosstalk detector, the charge amplitude of the true signal would be reduced, lowering the yield for the event and pushing it toward the nuclear recoil band. Additionally, the signal on the primary detector generated a small positive phonon pulse on the crosstalk detector, behavior that had not been previously observed, indicating that crosstalk occurs between phonon channels as well as charge channels. The phonon crosstalk resembles a charge signal, suggesting that it may be crosstalk between the charge and phonon channels that causes the positive phonon signal. It appears that many of these pulses are selected by the charge chi square cut and the cut that removes glitches, revealing that signals caused by crosstalk do not have the same shape as normal signals.

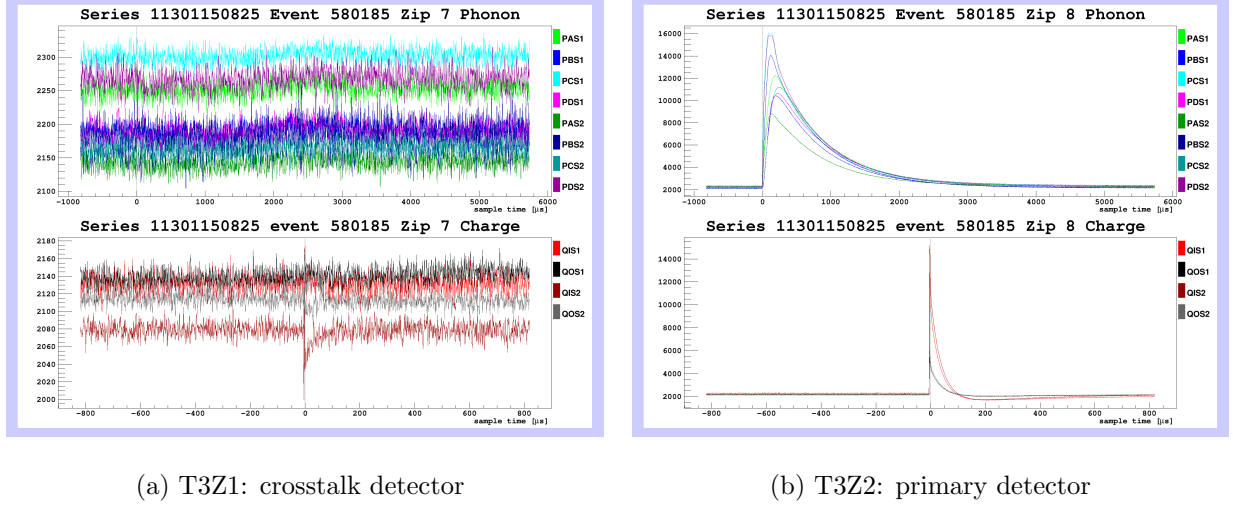


FIG. 6. Because no phonon crosstalk occurs on some low-energy events in the primary detector, the charge fitter does not have an accurate search window and can reconstruct the events as noise, placing them in a band along the primary axis as if no charge crosstalk were occurring between detectors. On this event in T3Z1, the charge signal was recorded as 1.52 keV, despite the clear negative pulse.

## 2. Noise-like events

It is unusual that certain events exhibit no crosstalk, clustering in a distinct band along the primary axis. The crosstalk should not distinguish between events, so while there can be a spread in the strength of the crosstalk due to natural variations in detector behavior, there should be a single, distinct trend. Figure 6 reveals that these events exhibit no phonon crosstalk above the level of noise (2 keV). As it is weaker than charge crosstalk, the smaller primary signals caused no visible phonon pulse. When the pulse-fitting algorithm searches for charge signals, it looks in a region approximately from  $-40 - 10 \mu\text{s}$  around the time when the phonon signal occurred. Since no phonon signal is recorded, the events reconstruct as noise on phonon and charge channels in many cases. Further evidence for this explanation can be observed in Figure 6(a). The charge value recorded on side 2 was 1.52 keV, but the charge signal is clearly negative. However, if the pulse was outside the window, the fitter would reconstruct a signal consistent with noise between  $-2$  and  $2$  keV. The events in the band along the axis are those whose phonon crosstalk was not strong enough to accurately set the search space for the charge fitter.

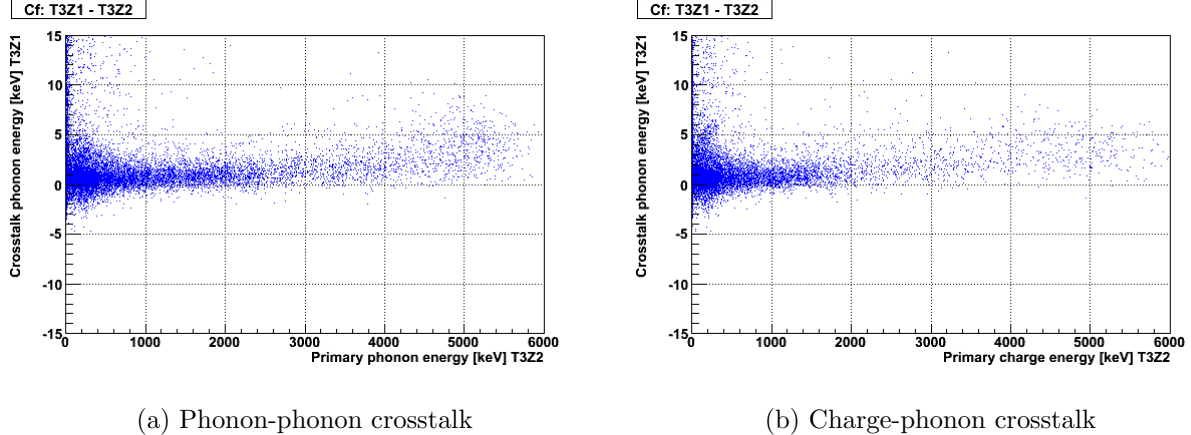


FIG. 7. A small positive phonon pulse is clearly evident in Figure 5, so there must be crosstalk occurring between phonon channels or between charge and phonon channels. In the plots above, we see noticeable positive slope of the bands that should lie along the primary axis. A rough estimate suggests that phonon crosstalk occurs on the orders of  $\sim 1\%$ . Thus, charge crosstalk will be the primary focus of investigation.

## B. Phonon crosstalk

Figure 5 confirmed that crosstalk was occurring between phonon channels as well as charge channels. The phonon-phonon and charge-phonon crosstalk planes are shown in Figure 7, where there are well-defined, positive slopes in both cases. Phonon crosstalk is particularly noticeable on pairs T3Z1-T3Z2 and T5Z1-T5Z2. These were also pairs that showed strong evidence of charge crosstalk in Figure 4. Thus, the strength of the phonon crosstalk appears to be related to the strength of the charge crosstalk, but its magnitude is smaller. Its strength, measured from the top of the crosstalk band, is typically about 0.1% of the primary signal. The initial crosstalk cut was developed to isolate instances where charge crosstalk has adverse effects.

## III. A CUT TO IDENTIFY CROSSTALK

The strength of the crosstalk between detectors was measured using  $^{252}\text{Cf}$  data because it provides the clearest bands for determining slope. Crosstalk strength was determined by estimating the slope along the lower edge of the crosstalk band. That is, the estimates represent the strongest crosstalk that occurs between detectors, and not the average amount

Detector pair <sup>a</sup>	Crosstalk (%)	Detector pair	Crosstalk (%)
T1Z1-Z2	0.5	T1Z2-Z1	0.2
T1Z2-Z3 <sup>b</sup>	n/a	T1Z3-Z2	n/a
T2Z1-Z2	0.2	T2Z2-Z1	0.3
T2Z2-Z3	0.3	T2Z3-Z2	0.5
T3Z1-Z2	0.6	T3Z2-Z1	0.3
T3Z2-Z3	0.3	T3Z3-Z2	0.2
T4Z1-Z2	0.5	T4Z2-Z1	0.2
T4Z2-Z3	0.4	T4Z3-Z2	0.4
T5Z1-Z2	0.4	T5Z2-Z1	unclear
T5Z2-Z3	0.2	T5Z3-Z2	0.3

<sup>a</sup> crosstalk-primary

<sup>b</sup> These detectors have many broken channels and will not be used to develop the crosstalk cut.

TABLE I. The charge crosstalk between all pairs of detectors given in strength of signal on crosstalk detector relative to the signal on the primary detector. It was measured based on the strongest crosstalk that occurred between detectors, from the bottom edge of the crosstalk band, to ensure that real crosstalk events would be selected. After these events are studied, the cut may be fine-tuned.

of crosstalk. Certain detectors appear to have crosstalk with parabolic energy dependence rather than linear energy dependence. Initially, the estimates were made by assuming all crosstalk was linear. For non-linear relationships, crosstalk was modeled as a line extending to the lowest point of the spread at 6 MeV on the primary detector.

## A. Cut definition

A cut was defined to remove events in which the amount of crosstalk from the primary detector exceeds 10% of the actual charge amplitude on the crosstalk detector. That is, it is first assumed that the measured charge,  $q_x$ , is reduced from its true amplitude by charge crosstalk equal to 10% of the charge amplitude and the value is corrected for the purposes of defining the cut. The earliest cut definition aims to over-select events rather than miss

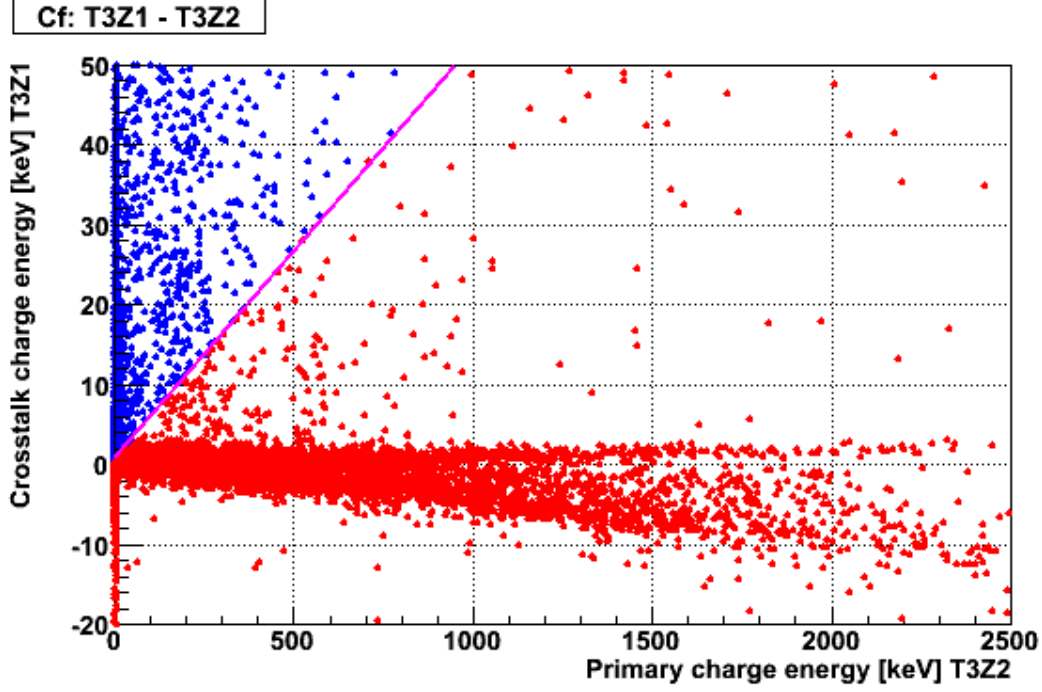


FIG. 8. The definition of the cut is shown in magenta, with all the failing values shown in red. The events of interest are those that fall just below the cut, when two events occur simultaneously but crosstalk from the primary detector reduces the charge on the crosstalk detector, pulling the event below the cut.

events, so the pulses can be studied directly before tuning the values used to define the cut on each detector. Given the crosstalk strength  $f$  measured in Table I, the cut can be defined

$$\frac{k}{1-k}q_x < fq_p \quad (2)$$

where  $k$  is the threshold for allowed reduction due to crosstalk (10%), and  $q_p$  is the charge on the primary detector. This identifies events that *are* affected by crosstalk. For detectors in the middle of a tower, the cut is calculated separately for the top and bottom primary detectors and then the two cuts are combined using a logical or operation. The cut definition is shown in Figure 9. To clarify, the events with negative charge amplitude that fall below the primary axis are not the events that the cut aims to select. They are singles or non-adjacent multiples that are used to measure the crosstalk strength. Barium multiples that are subject to crosstalk should fall just below the cut. These need to be identified when modeling the behavior of  $\gamma$ -interactions so they do not bias the analysis.

Detector	Consistency Region	$k = 0.05^a$	$k = 0.10^a$	$k = 0.15^a$
T1Z1	44	11 (25.0)	11 (25.0)	9 (20.5)
T1Z2 <sup>b</sup>	1771	n/a	n/a	n/a
T1Z3 <sup>b</sup>	1137	n/a	n/a	n/a
T2Z1	35	23 (65.7)	19 (54.3)	15 (42.9)
T2Z2	35	29 (82.9)	29 (82.9)	25 (71.4)
T2Z3	0	0 (n/a)	0 (n/a)	0 (n/a)
T3Z1	98	12 (12.2)	4 (4.1)	2 (2.0)
T3Z2	0	0 (n/a)	0 (n/a)	0 (n/a)
T3Z3	26	1 (3.8)	0 (0.0)	0 (0.0)
T4Z1	5020	807 (16.1)	388 (7.7)	260 (5.2)
T4Z2	5	1 (20.0)	0 (0.0)	0 (0.0)
T4Z3	31	23 (74.2)	19 (61.3)	17(54.8)
T5Z1	1953	67 (3.4)	22 (1.1)	8 (0.4)
T5Z2	7943	5 (0.1)	0 (0.0)	0 (0.0)
T5Z3	838	52 (6.2)	5 (0.6)	4 (0.5)

<sup>a</sup> values given represent number of events selected and (% of multiples selected)

<sup>b</sup> T1Z2 and T1Z3 have broken channels and will not be used in analysis.

TABLE II. The number of multiples events within the consistency region for all detectors, and the number of those that are identified as crosstalk for  $k = 0.05$ ,  $k = 0.10$ , and  $k = 0.15$ . The cut will use 10% as its threshold because the number of selected events does not vary greatly with a 5% change in either direction. This suggests that events are being selected accurately. There is no clear correlation between the selection rate and the crosstalk strength, another indication that the cut is effective.

## B. Performance

The cut was applied to  $^{133}\text{Ba}$  multiples that fall within the WIMP consistency region. To ensure that the number of events selected by the cut did not vary greatly with the threshold value,  $k$ , it was tested at 5% and 15% as well. Table II shows the number of events selected from the WIMP consistency region for  $^{133}\text{Ba}$  multiples. On most detectors, the selection

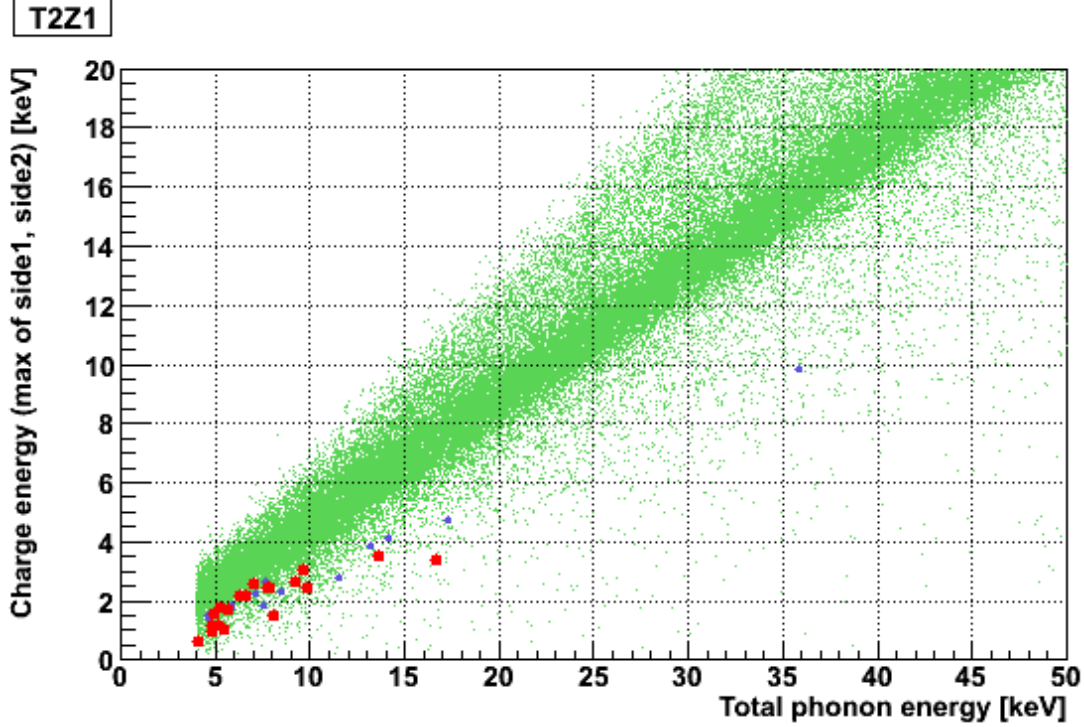
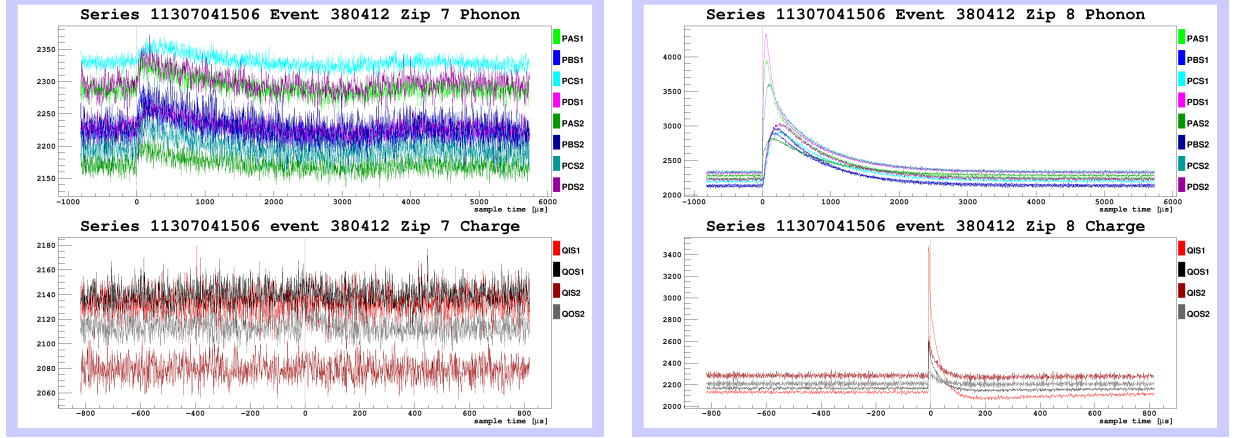


FIG. 9. All  $^{133}\text{Ba}$  events passing basic data quality cuts are shown in green. Blue events are those that fall within the barium consistency region; they pass the fiducial volume cuts and fall within the  $3\sigma$  nuclear recoil band. The events selected by the crosstalk cut are shown in red. Knowing that many of the events in the approximate WIMP search region fall there because of detector-generated crosstalk prevents the WIMP search region from becoming overly stringent by removing events unnecessarily.

rate does not vary greatly with the threshold value on detectors that do not contain broken channels and are likely to be used in analysis of low-background data. On detectors with broken channels, the crosstalk strength or threshold value may still be tuned to improve the robustness of the cut. Further improvements could be made on detectors that exhibited parabolic crosstalk relationships rather than linear relationships. The initial cut was defined by approximating all crosstalk with a line, but the cut's efficiency may be improved by implementing an energy-dependent crosstalk strength.

Additionally, aside from selecting low-energy events, the cut does not select events that are biased in relation to the fiducial volume cuts. In both the radial- and  $z$ -partition phase spaces, the crosstalk events are evenly distributed among the events passing all consistency cuts.



(a) T3Z1: crosstalk detector

(b) T3Z2: primary detector

FIG. 10. One of the four pulses identified as crosstalk in the consistency region of T3Z1.

#### IV. CONCLUSIONS

To understand the nature of  $\gamma$ -interactions in low-background data,  $^{133}\text{Barium}$  multiples are used as a proxy. However, since multiples occurring on adjacent detectors can have charge amplitude reduced by crosstalk between detectors, it is important to be able to identify these events and remove them, without removing all multiples events on adjacent detectors. Charge crosstalk occurs between adjacent detectors at the order of 0.5% or less, as expected. Phonon crosstalk also occurs, but at smaller scales than charge crosstalk (less than 0.1%). If the event on the primary detector is weak enough that the phonon crosstalk is not visible above 2 keV noise, the charge fitter search window may be defined so that it does not contain the crosstalk signal, and the event gets reconstructed as noise. We find that the shape of the signals generated solely by crosstalk (not a pulse with amplitude reduce due to crosstalk) often differs from a normal pulse, so it gets removed because it fails the charge chi square test or it gets removed by the quality cuts that identify glitch signals.

The crosstalk cut was defined by assuming that crosstalk was occurring at the maximum strength between detectors. The charge amplitude on the crosstalk detector is corrected to its true value assuming it had been reduced 10% by crosstalk. If 10% of the true charge amplitude is less than the crosstalk energy from the primary detector, the event is selected as a crosstalk event. The selection rate is robust against changes in the threshold parameter by 5% in either direction, suggesting that  $k = 0.1$  is a reasonable choice.



## ACKNOWLEDGMENTS

This work would not be possible without the efforts of internship coordinators Erik Ramberg and Roger Dixon. I would like to thank my mentor, Lauren Hsu, for her invaluable guidance throughout the summer as well as Dan Bauer, Ben Loer, and Ritoban Basu Thakur of the CDMS Collaboration. This work was supported in part by the U.S. Department of Energy, Office of Science, Office of Workforce Development for Teachers and Scientists (WDTS) under the Science Undergraduate Laboratory Internship (SULI) Program.

## REFERENCES

- <sup>1</sup>J. L. Feng, “Dark matter candidates from particle physics and methods of detection,” *Ann. Rev. Astron. Astrophys.* **48** (2010).
- <sup>2</sup>J. S. Gianfranco Bertone, Dan Hooper, “Particle dark matter: evidence, candidates and constraints,” *Physics Reports* **405** (2005).
- <sup>3</sup>J. P. Filippini, *A search for WIMP dark matter using the first five-tower run of the cryogenic dark matter search*, Ph.D. thesis, University of California, Berkeley (2008).
- <sup>4</sup>D. Clowe *et al.*, “A direct empirical proof of the existence of dark matter,” *Astrophys. J.* **648**, L109–L113 (2006).
- <sup>5</sup>*Particle Dark Matter: Observations, Models and Searches* (Cambridge University Press, 2010).
- <sup>6</sup>W. B. Atwood *et al.*, “The large area telescope on the Fermi Gamma-ray Space Telescope mission,” *Astrophys. J.* **697** (2009).
- <sup>7</sup>J. Yen, “Continued study on detector-detector charge x-talk,” (2013), an internal note from the SuperCDMS collaboration.
- <sup>8</sup>R. Agnese *et al.*, “Demonstration of surface electron rejection with interleaved germanium detectors for dark matter searches,” (2013), arXiv:1305.2405v3.
- <sup>9</sup>R. Agnese *et al.*, “Search for low-mass WIMPs with SuperCDMS,” *Phys. Rev. Lett.* **112** (2014).
- <sup>10</sup>Z. Ahmed *et al.*, “Dark matter search results from the CDMS II experiment,” *Science* **327** (2010).
- <sup>11</sup>R. W. Schnee, “Introduction to dark matter experiments,” (2011), arXiv:1101.5205v1.
- <sup>12</sup>J. Cherwinka *et al.*, “A search for the dark matter annual modulation in south pole ice,” *Astroparticle Physics* **35** (2012).